ARTICLE

Modeling Photovoltaic Performances of BTBPD-$PC_{61}BM$ System via Density Functional Theory Calculations

Cai-bin Zhao[a*], Zhi-hua Tang[a], Xiao-hua Guo[a], Hong-guang Ge[a*], Jian-qi Ma[a], Wen-liang Wang[b]

a. Shaanxi Key Laboratory of Catalysis, School of Chemical and Environmental Science, Shaanxi University of Technology, Hanzhong 723001, China
b. Key Laboratory for Macromolecular Science of Shaanxi Province, School of Chemistry and Chemical Engineering, Shaanxi Normal University, Xi'an 710062, China

(Dated: Received on February 16, 2017; Accepted on April 7, 2017)

Designing and fabricating high-performance photovoltaic devices have remained a major challenge in organic solar cell technologies. In this work, the photovoltaic performances of BTBPD-$PC_{61}BM$ system were theoretically investigated by means of density functional theory calculations coupled with the Marcus charge transfer model in order to seek novel photovoltaic systems. Moreover, the hole-transfer properties of BTBPD thin-film were also studied by an amorphous cell with 100 BTBPD molecules. Results revealed that the BTBPD-$PC_{61}BM$ system possessed a middle-sized open-circuit voltage of 0.70 V, large short-circuit current density of 16.874 mA/cm^2, large fill factor of 0.846, and high power conversion efficiency of 10%. With the Marcus model, the charge-dissociation rate constant was predicted to be as fast as 3.079×10^{13} s^{-1} in the BTBPD-$PC_{61}BM$ interface, which was as 3−5 orders of magnitude large as the decay (radiative and non-radiative) rate constant (10^8-10^{10} s^{-1}), indicating very high charge-dissociation efficiency (∼100%) in the BTBPD-$PC_{61}BM$ system. Furthermore, by the molecular dynamics simulation, the hole mobility for BTBPD thin-film was predicted to be as high as 3.970×10^{-3} cm^{2}V^{-1}s^{-1}, which can be attributed to its tight packing in solid state.

Key words: BTBPD, $PC_{61}BM$, Photovoltaic performances, Density functional theory

I. INTRODUCTION

In the past 100 years, with the overconsumption for fossil energies (coal, petroleum, and natural gas), environmental pollution problems have received widespread attention, and actively exploring for the clean and renewable energy has being become a hot and focus issue [1, 2]. As one of the most promising long-term solutions for the clean and renewable energy, free-metal photovoltaic technology has attracted intense interests in recent years due to its numerous advantages compared to the commercial inorganic photovoltaic technology, such as low manufacturing cost, flexibility, ease of solvent processing, and large-area capability [3−6]. Previous studies indicated that the high-performance donor materials should meet the following requirements: (i) narrow optical band gap, (ii) low-lying highest occupied molecular orbital (HOMO) level, and (iii) high hole carrier mobility [7−9]. Unfortunately, electron-donating materials that simultaneously satisfy those three demands are still scarce up to date.

Recently, Cai *et al.* synthesized a novel small molecule material (BTBPD) with the donor-acceptor-donor (D-A-D) character, and found that the thin-film field effect transistor fabricated with BTBPD had high hole mobility under natural ambient conditions [10]. More interestingly, BTBPD also exhibited the prominent capture to solar radiation, and its strongest absorption peak was found to red-shift to 696 nm in solid state. In a word, all properties suggest that BTBPD should be an excellent electron donor candidate. In this work, taking BTBPD as donor and [6,6]-phenyl-C_{61}-butyric acid methyl ester ($PC_{61}BM$) as acceptor, we carried out a systematic theoretical study on the photovoltaic properties for BTBPD-$PC_{61}BM$ system by means of quantum chemistry and molecular dynamics calculations coupled with the incoherent charge hopping model in order to seek novel high-performance photovoltaic systems. In this work, our main objectives are to theoretically explore the applicability of BTBPD as an electron-donating material and estimate the photovoltaic performances of BTBPD-$PC_{61}BM$ system. Theoretical calculations clearly show that BTBPD, as expected, is an excellent electron donor material, and the power conversion efficiency (PCE) of BTBPD-$PC_{61}BM$ system theoretically reaches up to 10%.

*Authors to whom correspondence should be addressed. E-mail: zhaocb@snut.edu.cn, gehg@snut.edu.cn, Tel.: +86-916-2641660

 ©2017 Chinese Physical Society

II. COMPUTATIONAL METHODS

To simplify calculations, the long-alkyl chain (2-ethylhexyl) in BTBPD was replaced with the CH_3, because it has been confirmed that the substituted alkyl in organic compounds has hardly any effect on their electronic structure and optical properties, and merely promotes solubility [11−13]. All stable species were fully optimized without any symmetry constraints by means of density functional theory (DFT) calculations with the B3LYP hybrid functional [14] and the 6-31G(d) basis set, with subsequent frequency calculations to confirm that they were true minima of potential energy surface. Based on the optimized geometries, the UV-Vis spectrum for BTBPD was simulated with the time-dependent density functional theory (TD-DFT) [15, 16] and the B3LYP/6-31G(d) scheme. In order to determine the most reasonable geometry of BTBPD-$PC_{61}BM$ complex, the detailed potential-surface scan was carried out between $PC_{61}BM$ and BTBPD with the CAM-B3LYP-D3(BJ)/6-31G(d) method [17, 18]. As seen in FIG. S1 (supplementary materials), the BTBPD-$PC_{61}BM$ complex was found to be the most stable when the centroids distance of $PC_{61}BM$ and BTBPD is at 8.0 Å, which is in good agreement with the recent studies [19, 20]. Then, in subsequent calculations, the centroids distance of $PC_{61}BM$ and BTBPD was invariably fixed at 8.0 Å. In addition, in this work the influence of molecular orientation was also considered. As is shown in FIG. S2 (supplementary materials), the molecular orientation affects a little on the BTBPD-$PC_{61}BM$ complex. Based on optimized structures for $PC_{61}BM$, BTBPD, and BTBPD-$PC_{61}BM$ complex, total density of states (TDOS) and partial density of states (PDOS) were visualized with the Multiwfn 3.3.6 software developed by Lu *et al.* [21, 22]. All quantum chemistry calculations were carried out with the Gaussian 09 software [23].

III. RESULTS AND DISCUSSION

A. Photovoltaic performances of BTBPD-$PC_{61}BM$ system

1. Electronic properties and open circuit-voltage

BTBPD and $PC_{61}BM$ molecular structures are depicted in FIG. 1. The geometric optimization revealed that BTBPD molecule has a near planar conformation (FIG. S3 in supplementary materials), and the dihedral angle (α) between its adjacent units is close to 20°, which indicates its good π-conjugated character. FIG. 2 shows the TDOS and PDOS of $PC_{61}BM$, BTBPD, and BTBPD-$PC_{61}BM$ complex. With the DOS, it is very easy to directly observe the contribution from each substituent to the frontier molecular orbital (FMO). As seen, in $PC_{61}BM$ molecule all density of

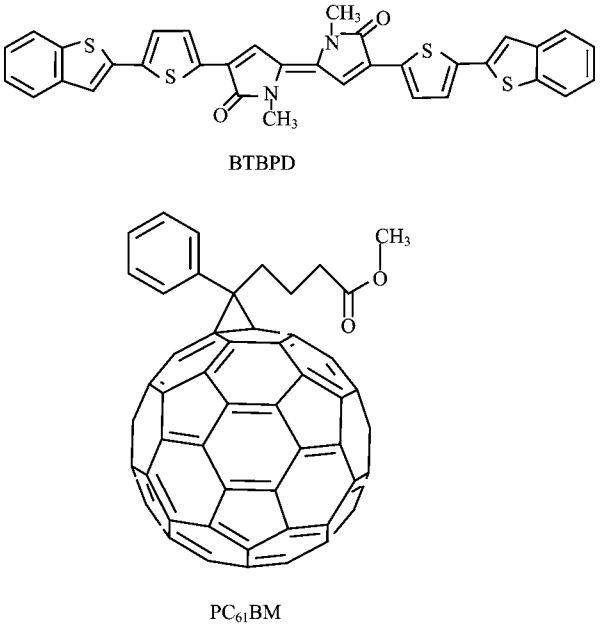

FIG. 1 Molecular structures of BTBPD and $PC_{61}BM$.

HOMOs and LUMOs was found to concentrate on the C_{60} sphere in the energy range from −10.0 eV to 2.0 eV, and the contribution from the substituent (methyl-4-phenylbutanoate) is very small, meaning the substituent only enhances the C_{60} solubility, and has a little influence on its electronic properties, which agrees well with the previous experimental studies [24, 25]. Moreover, it can be noticed that CH_3 contributes very small to the HOMO and LUMO in BTBPD molecule, verifying it is rational to replace 2-ethylhexyl with CH_3 in the current work. Interestingly, the benzo[b]thiophene (BT) and bipyrrolylidene-2,2′(1H,1′H)-dione (BPD) in BTBPD molecule contribute very much to both the HOMO and the LUMO, denoting the HOMO and LUMO of BTBPD delocalize over the molecular skeleton, rather than centralize at a certain molecular fragment, which benefits the rapid charge-transfer between two molecules. As for BTBPD-$PC_{61}BM$ complex, the HOMO and the LUMO exhibit an obvious separation characteristic, and the HOMO completely locates on the BTBPD, while the LUMO mainly centuries on the $PC_{61}BM$, which suggests the easy formation of $BTBPD^{\cdot+}$-$PC_{61}BM^{\cdot-}$ charge-separated state. According to the previous study, the open circuit-voltage for organic solar cells (OSCs), V_{oc}, can be estimated with [26]:

$$V_{oc} = \frac{1}{e}\left(|E_{HOMO}\,(D)| - |E_{LUMO}\,(A)|\right) - 0.3 \qquad (1)$$

where E_{HOMO}(D) and E_{LUMO}(A) are the HOMO level of donor and the LUMO level of $PC_{61}BM$, e is the electron charge, and the value of 0.3 is an empirical factor. Then, based on the experiment HOMO (−5.0 eV [10]) for BTBPD and LUMO (−4.0 eV [27, 28]) for

DOI:10.1063/1674-0068/30/cjcp1702016 ©2017 Chinese Physical Society

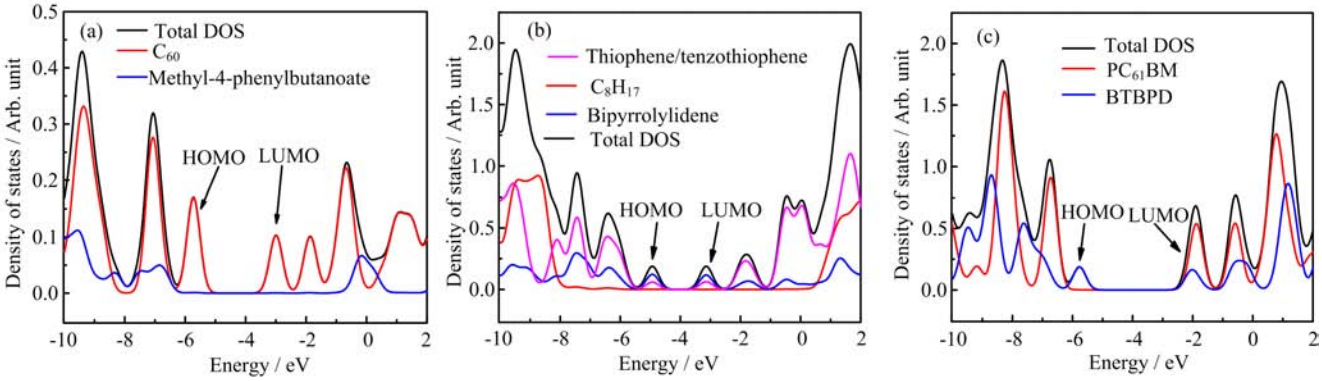

FIG. 2 Total density of states and partial density of states of (a) $PC_{61}BM$, (b) BTBPD, and (c) $PC_{61}BM$-BTBPD complex.

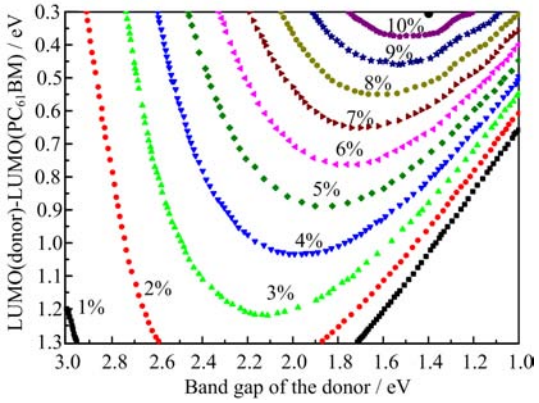

FIG. 3 Predicted PCE for BTBPD-$PC_{61}BM$ cell with the Scharber diagram.

$PC_{61}BM$, the V_{oc} was estimated to be as large as 0.70 V for BTBPD-$PC_{61}BM$ system. More interestingly, the PCE of BTBPD-$PC_{61}BM$ system was predicted to be over 10% (FIG. 3) by means of the Scharber diagram, indicating the BTBPD-$PC_{61}BM$ system is a promising OSC candidate.

2. Charge binding energy and optical absorption properties

As is well-known, the charge binding energy (E_b) is one of the most parameters in photovoltaic devices, which is directly related to the charge separation. Usually E_b is taken as the difference between the transport gap (E_t) and the optical band gap (E_{opt}). The former is the difference between the adiabatic ionization potential (E_{AIP}) and electron affinity (E_{AEA}) of donor in the solid state, while the latter is taken as the first-singlet emission energy (E_m). Then, the E_b can be calculated as the following expression [29]:

$$E_b = E_{AIP} - E_{AEA} - E_m \quad (2)$$

As seen in Eq.(2), to calculate E_b, the E_{AIP} and E_{AEA} of donor in solid state firstly should be calculated. Here,

TABLE I Calculated E_{AIP}, E_{AEA}, and E_b values in the gas and solid state for BTBPD with two different DFT methods.

Method	State	E_{AIP}	E_{AEA}	E_b
B3LYP/6-31G(d,p)	Gas	5.483	1.982	1.596
	Solid	4.779	2.951	0.594
	P_+/P_- [a]	0.704	0.969	
CAM-B3LYP/6-31G(d,p)	Gas	5.761	1.851	1.733
	Solid	5.020	2.909	0.675
	P_+/P_- [a]	0.741	1.058	

[a] P_+/P_- represents the cation/anion polarization energy.

the E_{AIP}/E_{AEA} of solid BTBPD was estimated via the scheme reported by Schwenn *et al.* [30], which has been verified to be an excellent selection that estimates the electronic properties of organic materials in the solid state. Table I shows calculated E_{AIP} and E_{AEA} values for BTBPD in gas phase and solid state with two different DFT methods. It can be noted that E_b estimated by two methods is as large as 1.596 and 1.733 eV in gas phase, which is much larger compared with those measured values of 0.2−1.0 eV in many organic materials [31], which can be attributed to the solid stacking effect. Comparing the results in gas phase to the ones in solid state, it can be noticed that in gas phase E_{AIP} is larger, while E_{AEA} is smaller, which is similar to the measured and theoretical results in acenes [32]. According to the calculated E_{AIP}, E_{AEA}, and E_m for the solid BTBPD, the E_b was estimated to be about 0.594 eV. The precious study showed that the exciton is unstable when $E_b < k_BT$, which amounts to 0.025 eV at room temperature [33]. According to the calculated E_b for BTBPD, it can be deduced that the photo-induced exciton in BTBPD is relatively stable, which can be efficiently transported to the BTBPD-$PC_{61}BM$ interface without rapidly being decayed in transit.

As is known to all, the good harvest for solar radiation is essential for efficient dye sensitizers, which determines the short-circuit current density J_{sc} of DSC de-

DOI:10.1063/1674-0068/30/cjcp1702016 ©2017 Chinese Physical Society

TABLE II Calculated excited energies (λ_{max}), molar absorption coefficients (ε), oscillator strengths (f), and main configuration for BTBPD with different DFT methods coupled with the 6-31G(d,p) basis set.

Method	State	λ_{max}/nm	λ_{max}/eV	ε/(L·mol^{-1}cm^{-3})	f	Main configuration
B3LYP	$S_0 \rightarrow S_1$	693	1.790	56585	1.3963	HOMO→LUMO(100%)
CAM-B3LYP	$S_0 \rightarrow S_1$	617	2.008	52720	1.3017	HOMO→LUMO(96%)
M062X	$S_0 \rightarrow S_1$	623	1.991	52387	1.3489	HOMO→LUMO(97%)
MPW1PW91	$S_0 \rightarrow S_1$	682	1.818	56535	1.3956	HOMO→LUMO(100%)
PBE0	$S_0 \rightarrow S_1$	788	1.573	53866	1.3105	HOMO→LUMO(100%)
TPSSh	$S_0 \rightarrow S_1$	769	1.612	56496	1.3787	HOMO→LUMO(100%)
ωB97XD	$S_0 \rightarrow S_1$	610	2.033	50245	1.2406	HOMO→LUMO(93%)
LC-ωPBE	$S_0 \rightarrow S_1$	562	2.205	49731	1.2279	HOMO→LUMO(90%)
Expt. [10]		696	1.782	53000		

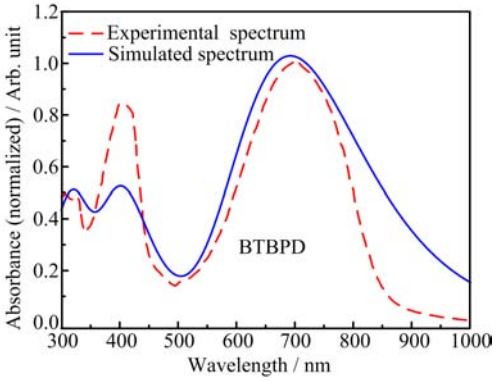

FIG. 4 Simulated and experimental absorption spectra for BTBPD in solid state.

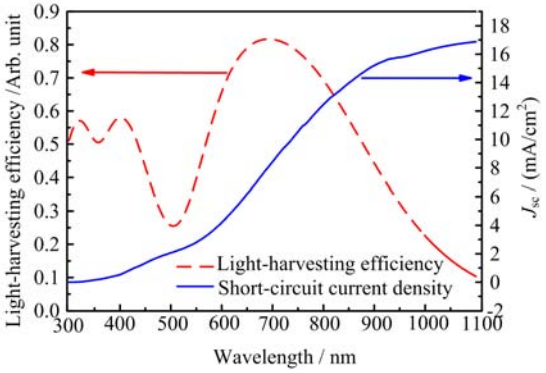

FIG. 5 Predicted J_{sc} and η_λ for BTBPD-$PC_{61}BM$ cell.

vices to some extent. To explore reliable DFT methods estimating optical absorption properties for BTBPD, a set of popular DFT methods were tested. As seen in Table II, compared with the experimental value, the B3LYP hybrid functional can estimate accurately the excited energy of BTBPD, and the derivation between the theoretical and experimental values is only about 3.0 nm (about 0.008 eV). Moreover, it can be noticed that the strongest absorption in UV-Vis spectrum for the BTBPD molecule can be assigned to the π-π^* type, and dominated completely by the electron transition of HOMO→LUMO (∼100%). In addition, as observed in FIG. 4, the TD-B3LYP/6-31G(d) method can reproduce well the UV-Vis spectrum of BTBPD molecule in solid state, which confirms again the method reliability used in this work. Since the HOMO and LUMO for BTBPD distribute the whole molecule skeleton (FIG. S4 in supplementary materials), the lowest-excited singlet is a typically local excited state, and no obvious charge is transferred in light absorption process.

3. Short-circuit current density J_{sc}, fill factor FF, and PCE η

Short-circuit current density J_{sc} is another key parameter that determines the PCE of OSC devices, which can be expressed as [34, 35]:

$$J_{sc} = q \int_0^\infty \eta_{EQE}(\lambda) \times S(\lambda) d\lambda \quad (3)$$

where $S(\lambda)$ is incident photon-to-current conversion efficiency at a fixed wavelength, e is the unit charge, and $\eta_{EQE}(\lambda)$ is the external quantum efficiency. The $\eta_{EQE}(\lambda)$ term can be described as the product of η_λ (light-harvesting efficiency), η_{CT} (charge transfer efficiency), and η_{coll} (charge collection efficiency) [36],

$$\eta_{EQE} = \eta_\lambda \eta_{CT} \eta_{coll} \quad (4)$$

where η_λ can be calculated as η_λ=1−10^{-f}, f is the oscillator strength. Then, to estimate the maximum J_{sc}, we sent the η_{CT}=1.0 and the η_{coll}=1.0. Our calculation showed that f is about 1.3963 at the lowest-excited singlet state for BTBPD, then yielding the η_λ=0.752. FIG. 5 shows that the simulated η_λ and J_{sc} with the above-mentioned parameters. As seen, the J_{sc} was estimated to be as high as 16.874 mA/cm^2 for the BTBPD-$PC_{61}BM$ system, which can be attributed to its strong spectral response. In addition, it can be noticed that the η_λ is as large as 81.7% in visible region. Relatively, BTBPD has a weak capture for ultraviolet radiation (η_λ≈57%). For the FF calculation, an approximate scheme can be expressed as [37, 38],

DOI:10.1063/1674-0068/30/cjcp1702016 ©2017 Chinese Physical Society

$$FF = \frac{\nu_{oc} - \ln(\nu_{oc} + 0.72)}{\nu_{oc} + 1} \quad (5)$$

where ν_{oc} is the dimensionless voltage, which can be estimated with the V_{oc} [39, 40],

$$\nu_{oc} = \frac{qV_{oc}}{nk_BT} \quad (6)$$

where k_B, T and q are Boltzmann constant, temperature (here, we set T=300 K), and elementary charge respectively, n is an ideality factor relating to an ideal (n=1) or non-ideal (n>1) diode [41], organic solar cells typically have ideality factors in the range of 1.5−2.0 due to their inherent disorder [42]. According to the calculated V_{oc} (0.70 V) for the BTBPD-$PC_{61}BM$ system, the ν_{oc} was estimated to be 27.08 at n=1.0 and 13.54 at n=2, then, the FF for $P_{61}BM$-BTBPD was predicted to be as high as 0.748 (n=2.0) and 0.846 (n=1.0), in excellent agreement with measured values in most OSC devices. According to the previous study, the PCE (η) of OSC devices can be estimated with the following equation [43, 44]

$$\eta = \frac{P_{max}}{P_{in}} = \frac{V_{oc}J_{sc}}{P_{in}}FF \quad (7)$$

where P_{max} and P_{in}(=100 mW/cm^2) are the maximum and incident power respectively. With the calculated V_{oc}, J_{sc}, and FF, the PCE of BTBPD-$PC_{61}BM$ system was predicted to be 8.83% (n=2.0) and 9.99% (n=1.0), which is slightly smaller than the value (>10%) estimated by the Scharber diagram.

B. Charge dissociation and recombination rates

Generally, the charge transfer in organic photoelectric materials obeys the incoherent charge-hopping mechanism, and the transfer rate constant between donor and acceptor, k_{DA}, can be evaluated via the Marcus model [45, 46],

$$k_{DA} = \frac{2\pi}{h}\sqrt{\frac{\pi}{\lambda k_BT}}\,|V_{DA}|^2 \exp\left[-\frac{(\Delta G + \lambda)^2}{4\lambda k_BT}\right] \quad (8)$$

where λ is the total reorganization energy, V_{DA} is the effective charge transfer integral between donor and acceptor, ΔG is the Gibbs free energy change between the initial and final states, k_B is Boltzmann constant, h is Planck constant, and T is the temperature (here, we set T=300 K).

1. Gibbs free energy change in charge dissociation and recombination

As seen in Eq.(8), the Gibbs free energy change, ΔG, has a remarkable influence on the k_{DA}. Generally, the ΔG can be estimated as the energy difference in the final and initial states, accounting for the Coulombic attraction between the two charges in charge-separated state. Thus, for the charge-dissociation, the ΔG is written as [47],

$$\Delta G_{dis} = E_D^+(Q^+) + E_A^-(Q^-) - E_D^*(Q^*) - E_A^0(Q^0) + \Delta E_{coul} \quad (9)$$

where $E_D^*(Q^*)$ and $E_D^+(Q^+)$ is the total energy of isolated donor in its equilibrium geometry of lowest singlet-excited and cationic state, $E_A^-(Q^-)$ and $E_A^0(Q^0)$ are the total energies of isolated acceptor in its equilibrium geometries of anionic and ground states, ΔE_{coul} is the Coulombic attraction between donor and acceptor in charge-separated state, which can be estimated with the flowing equation,

$$\Delta E_{coul} = \sum_{D^+}\sum_{A^-}\frac{q_{D^+}q_{A^-}}{4\pi\varepsilon_0\varepsilon_s r_{D^+A^-}} - \sum_{D^*}\sum_{A}\frac{q_{D^*}q_{A}}{4\pi\varepsilon_0\varepsilon_s r_{D^*A}} \quad (10)$$

where q_D and q_A are the atomic charges on donor and acceptor in their relevant states with a separation distance, r_{DA}. The ε_0 is the vacuum dielectric constant (8.854×10^{-12} F/m), and the ε_s is the static dielectric constant of medium. Similarly, the Gibbs free energy change (ΔG_{rec}) in charge recombination can also be estimated with the expression similar to Eq.(9) and Eq.(10). Here, the ε_s is estimated with the Clausius-Mossotti equation [48],

$$\varepsilon_s = \left(1 + \frac{8\pi\overline{\alpha}}{3V}\right)\left(1 - \frac{4\pi\overline{\alpha}}{3V}\right)^{-1} \quad (11)$$

where V is the Connolly molecular volume, $\overline{\alpha}$ is the isotropic component of molecular polarizability, $\overline{\alpha}$=1/3$\sum_i \alpha_{ii}$, and the α_{ii} is the diagonal matrix elements of first-order polarizability tensor. Calculations show that the ε_s is 3.653 for BTBPD, which is in accord with the measured values (ranging from 2.0 to 5.0 [49, 50]) in most organic materials. As for $PC_{61}BM$, the experimental ε_s value of 3.9 [51] was used in this work. The total ε_s of BTBPD-$PC_{61}BM$ system was taken as an average of their respective contributions. Our calculation showed that the ΔG_{dis} is about −0.316 eV, while the ΔG_{rec} is smaller (−0.640 eV). As seen, the ΔG_{dis} and ΔG_{rec} are consistently calculated to be negative, denoting that the charge-dissociation and charge-recombination are always favorable in thermodynamics. In addition, the smaller ΔG_{rec} indicated a larger driving force in charge-recombination process.

2. Reorganization energies in charge dissociation and recombination

Generally, in organic solids the total reorganization energy (λ) of electron transfer can be divided into two parts, namely the internal reorganization energy (λ_{int})

DOI:10.1063/1674-0068/30/cjcp1702016 ©2017 Chinese Physical Society

and the external one (λ_{ext}). The λ_{int} term can be calculated with the adiabatic potential energy surface (PES) method [52, 53]. In the case of charge dissociation, the λ_{int} is actually taken as an average of the following λ_1 and λ_2 [54],

$$\lambda_1 = (E_D^*(Q^+) + E_A^0(Q^-)) - (E_D^*(Q^*) + E_A^0(Q^0)) \quad (12)$$

$$\lambda_2 = (E_D^+(Q^*) + E_A^-(Q^0)) - (E_D^+(Q^+) + E_A^-(Q^-)) \quad (13)$$

where $E_D^*(Q^+)$ and $E_D^*(Q^*)$ are the energies of donors in the lowest excited-state with the equilibrium geometries of cationic and excited state respectively, $E_D^+(Q^*)$ and $E_D^+(Q^+)$ are the energies of donors in the cationic states with the equilibrium geometries of excited and cationic states respectively, $E_A^0(Q^-)$ and $E_A^0(Q^0)$ are the energies of acceptors in the neutral states with the equilibrium geometries of anion and neutral states, respectively, and $E_A^-(Q^0)/E_A^0(Q^-)$ are the energies of acceptors in the anionic states with the equilibrium geometries of neutral and anionic states. As seen in Table III, our calculation showed that the λ_{int} (λ_{dis}) is 0.191 eV in charge-dissociation process for BTBPD-$PC_{61}BM$, which remarkably increases to 0.348 eV in the case of charge recombination. Compared with the λ_{int}, the λ_{ext} was difficult to be accurately calculated. Here, we used the classical dielectric continuum model initially developed by Marcus for the electron-transfer reaction between spherical ions in solution to estimate the λ_{ext}. According to this model, the λ_{ext} term is given by [55],

$$\lambda_{ext}=\frac{(\Delta e)^2}{8\pi\varepsilon_0}\left(\frac{1}{\varepsilon_{op}}-\frac{1}{\varepsilon_s}\right)\left(\frac{1}{R_D}+\frac{1}{R_A}-2\sum_D\sum_A\frac{q_D q_A}{r_{DA}}\right) \quad (14)$$

where ε_{op} is the optical dielectric constant of medium, R_D (=6.41 Å for BTBPD) and R_A (=6.50 Å for $PC_{61}BM$) are the effective radii of donor and acceptor estimated as the radius of sphere having the same surface as the surface accessible area of molecule. The q_D and q_A denote the atomic charges on the ions. The ε_{op} which can be estimated with the Lorentz-Lorenz equation [56, 57],

$$\varepsilon_{op} = n^2 = \frac{V_m + 2R}{V_m - R} \quad (15)$$

where n is the refractive index, V_m is the molar volume (V_m=M/ρ, M is the molar mass, and ρ is the density of material), R is the molar refraction. Here, the ρ was estimated with the molecular dynamics method, and the simulated detail was shown in the supplementary materials. Our results showed the ε_{op} and ρ for BTBPD were equal to 2.960 and 1.312 g/cm^3 respectively. As for $PC_{61}BM$, the experimental refractive index (n=1.866) is used to estimate to the ε_{op}, which is equal to 3.482 according to our estimation. With the above-mentioned parameters, the λ_{ext} can be conveniently obtained. At the case of BTBPD-$PC_{61}BM$, the λ_{ext} is equal to 0.103 eV. Summary, the λ is 0.294 eV in charge-dissociation process for BTBPD-$PC_{61}BM$ system, which remarkably increases to 0.451 eV for the charge-recombination process.

TABLE III Calculated λ_{dis}, λ_{rec}, and λ_{ext} values in the gas and solid state for BTBPD with two different DFT methods.

Method	State	λ_{dis}	λ_{rec}	λ_{ext}
B3LYP/6-31G(d,p)	Gas	0.288	0.364	0.103
	Solid	0.191	0.348	0.103
CAM-B3LYP/6-31G(d,p)	Gas	0.248	0.550	0.103
	Solid	0.214	0.518	0.102

3. Charge transfer integral in charge dissociation and recombination

As seen in Eq.(8), the V_{DA} is an important parameter that determines the k_{DA}, in this work, the direct-coupling (DC) method coupled with the PW91PW91/6-31G(d) scheme was used to estimate V_{DA} [58, 59], which have been illustrated to present the most accurate V_{DA} value at the DFT level [60, 61]. In terms of the DC scheme, the V_{DA} value of charge transfer can be calculated by the following expression [62],

$$V_{D(i)A(j)} = \frac{T_{D(i)A(j)} - 0.5(e_{D(i)} + e_{A(j)})S_{D(i)A(j)}}{1 - S^2_{D(i)A(j)}} \quad (16)$$

where $T_{D(i)A(j)}$ is the charge transfer integral of the ith molecular orbital of donor and the jth molecular orbital of acceptor, $S_{D(i)A(j)}$ is the spatial overlap integral of the above two molecular orbitals, and $e_{D(i)}/e_{A(j)}$ is the site energy. $T_{D(i)A(j)}$, $S_{D(i)A(j)}$, and $e_{D(i)}/e_{A(j)}$ can be obtained from the $T_{D(i)A(j)}$=$\langle\psi_{D(i)}|F^{KS}|\psi_{A(j)}\rangle$, $S_{D(i)A(j)}$=$\langle\psi_{D(i)}|\psi_{A(j)}\rangle$, and $e_{D(i)}/e_{A(j)}$=$\langle\psi_{D(i)}|\psi_{A(j)}|F^{KS}|\psi_{D(i)}|\psi_{A(j)}\rangle$. Among them, $\psi_{D(i)}$ is the HOMO (for charge-recombination) or LUMO (for charge-dissociation) of donor, $\psi_{A(j)}$ is the LUMO of acceptor, and F^{KS} is the Kohn-Sham matrix of donor-acceptor system. The F^{KS} can be obtained from

$$F^{KS} = SC\varepsilon C^{-1} \quad (17)$$

where S is the intermolecular overlap matrix, C is the molecular orbital coefficient matrix from the isolated monomer, and ε is the orbital energy from one-step diagonalization without iteration. Generally, the V_{DA} in the charge-dissociation process is taken as the coupling between the LUMO of donor and acceptor. However, since the LUMO+1 and LUMO+2 in $PC_{61}BM$ are degenerated energetically with its LUMO [63], the V_{DA} between the LUMO of BTBPD and the LUMO+1/LUMO+2 of $PC_{61}BM$ was also computed. Finally, the average V_{DA} value ($(V_1V_2V_3)^{1/3}$)

DOI:10.1063/1674-0068/30/cjcp1702016 ©2017 Chinese Physical Society

was viewed as the total V_{DA} and then applied to estimate the charge-dissociation rate. As for the charge-recombination, the same treatment was done. Calculations show that the V_{DA} in the charge dissociation for the BTBPD-$PC_{61}BM$ is −31.82 meV, which is equal to 20.37 meV for the charge-recombination process. Based on the calculated λ and V_{DA} values, the charge-dissociation (k_{dis}) and charge-recombination (k_{rec}) rate constants were estimated to be as high as 3.079×10^{13} and 4.808×10^{12} s^{-1} respectively in BTBPD-$PC_{61}BM$ complex. Recent studies illustrated that the decay rate constant (k_d) of excited organic molecules typically ranges 1.0×10^{8} s^{-1} to 1.0×10^{10} s^{-1} [64]. Our results showed that the k_{dis} is larger than the k_d 3−5 orders of magnitude, which indicates high charge-dissociation efficiency (∼100%) in the BTBPD-$PC_{61}BM$ system. In addition, although the k_{rec} is relatively large, the charge-recombination efficiency is still very low. According to previous studies, the electron transferred onto $PC_{61}BM$ can be rapidly converted to the triplet state from the singlet state [63, 64], which remarkably hinders from the recombination of free carriers.

C. Hole transfer rate and hole mobility in BTBPD thin-film

As is known to all, the charge transport ability of donor remarkably affects the solar cell's performance. Thus, it is essential to discuss charge transport properties of BTBPD thin-film. Generally, the charge transport ability of organic materials can be chartered with its carrier mobility, μ, which can be calculated by means of the Einstein-Smoluchowski equation [67, 68],

$$\mu = \frac{eD}{k_B T} \tag{18}$$

where D is diffusion coefficient, e is elementary charge, k_B is Boltzmann constant, and T is absolute temperature, respectively. The D can be estimated by means of the following appropriate relation [69, 70]:

$$D \approx \frac{1}{2n}\sum_i d_i^2 k_i P_i \tag{19}$$

where n is the spatial dimensionality, which is 3 in organic solids, d_i is the centroids distance of the ith hopping dimer, k_i is the charge transfer rate constant, and P_i is the hopping probability, $P_i{=}k_i/\sum_i k_i$. In this work, the charge mobility of BTBPD thin-film was evaluated by means of an amorphous cell with 100 BTBPD molecules built by means of the molecular dynamics simulation. Table IV lists the calculated the λ_{int} term with two different DFT methods. As seen, the CAM-B3LYP/6-31G(d,p) scheme presents quite large λ_{int} values due to the long-range correlation effect. In addition, it can be noticed that the λ_{int} in solid state is obviously smaller than that in gas phase, denoting that the solid stack to some extent, limits the structural relaxation of BTBPD molecule in charge transfer process. Since the donor materials in OSC devices usually keep in solid state under operating conditions, the λ_{int} estimated in the solid state is more reasonable. To explore possible charge transfer dimers, 21 molecular pairs with the relatively large V_{DA} values were abstracted from the optimized amorphous cell, and their geometries, centroids distances, as well as estimated V_{DA} values were shown in Table S1 (supplementary materials). Based on the λ_{int} the solid state and V_{DA} values, the hole carrier mobility, μ_h, was estimated to be as high as 3.970×10^{-3} $cm^2V^{-1}s^{-1}$ in the solid BTBPD, which is in excellent agreement with its measured value (3.0×10^{-3}−8.4×10^{-3} $cm^2V^{-1}s^{-1}$ [10]. According to the previous investigation, for high-performance OSC devices, the μ_h should be not less than 10^{-3} $cm^2V^{-1}s^{-1}$ [26]. Our estimation showed as a potential donor material of OSC devices, the BTBPD can rapidly transports holes.

TABLE IV Calculated λ_{int} for BTBPD in solid and gas states with two different DFT methods.

Method	State	λ_1	λ_2	λ_{int}
B3LYP/6-31G(d,p)	Gas	0.188	0.232	0.420
	Solid	0.175	0.213	0.388
CAM-B3LYP/6-31G(d,p)	Gas	0.415	0.377	0.792
	Solid	0.378	0.349	0.727

IV. CONCLUSION

In summary, BTBPD-$PC_{61}BM$ as a promising OSC system was theoretically studied by means of quantum-chemical and molecular dynamics calculations. Results showed that BTBPD-$PC_{61}BM$ system possesses middle-sized open-circuit voltage (0.7 V), large short-circuit current density (16.874 mA/cm^2), high fill factor (0.846), and high PCE (>10%). In addition, BTBPD was also revealed to possess the strong optical response, and suitable charge-binding energy (0.457 eV). Using the Marcus model, the k_{dis} was estimated to be as large as 3.079×10^{13} s^{-1} in the BTBPD-$PC_{61}BM$ blend, which indicated very high charge-dissociation efficiency. Moreover, by means of an amorphous cell model with 100 BTBPD molecules, the hole carrier mobility of BTBPD thin film was predicted to be as high as 3.970×10^{-3} $cm^2V^{-1}s^{-1}$. In brief, our calculation shows that BTBPD is a very potential donor material, and the BTBPD-$PC_{61}BM$ system is a high-performance OSC candidate. However, these results need to be verified by experiments.

Supplementary material: Detailed potential-surface scan, optimized BTBPD geometry, calculated the lowest-excited energy for BTBPD, HOMO and LUMO

DOI:10.1063/1674-0068/30/cjcp1702016 ©2017 Chinese Physical Society

of BTBPD, and detailed description for molecular dynamics simulation are shown.

V. ACKNOWLEDGEMENTS

This work was supported by the National Natural Science Foundation of China (No.21373132, No.21502109, No.21603133), the Education Department of Shaanxi Provincial Government Research Projects (No.16JK1142, No.16JK1134), and the Scientific Research Foundation of Shaanxi University of Technology for Recruited Talents (No.SLGKYQD2-13, No.SLGKYQD2-10, No.SLGQD14-10).

[1] A. M. Bagher, Sust. Energy. **2**, 85 (2014).
[2] O. Ellabbana, H. Abu-Rub, and F. Blaabjerg, Renew. Sust. Energy. Rev. **39**, 748 (2014).
[3] A. Hagfeldt, G. Boschloo, L. Sun, L. Kloo, and H. Pettersson, Chem. Rev. **110**, 6595 (2010).
[4] M. T. Spitler and B. A. Parkinson, Acc. Chem. Res. **42**, 2017 (2009).
[5] S. Lewis, Science **315**, 798 (2007).
[6] M. Grätzel, Acc. Chem. Res. **42**, 1788 (2009).
[7] J. Peet, M. L. Senatore, A. J. Heeger, and G. C. Bazan, Adv. Mater. **21**, 1521 (2009).
[8] M. C. Scharber, D. Mhlbacher, M. Koppe, P. Denk, C. Waldauf, A. J. Heeger, and C. J. Brabec, Adv. Mater. **18**, 789 (2006).
[9] P. Sista, H. Nguyen, J. Murphy, J. Hao, D. K. Dei, K. Palaniappan, J. Servello, R. S. Kularatne, B. E. Gnade, B. Xue, P. C. Dastoor, M. C. Biewer, and M. C. Stefan, Macromolecules **43**, 7875 (2010).
[10] Z. Cai, Y. Guo, S. Yang, Q. Peng, H. Luo, Z. Liu, G. Zhang, Y. Liu, and D. Zhang, Chem. Mater. **25**, 471 (2013).
[11] Y. Yi, V. Coropceanu, and J. L. Brédas, J. Mater. Chem. **21**, 1479 (2011).
[12] T. Liu, J. S. Gao, B. H. Xia, X. Zhou, and H. X. Zhang, Polymer **48**, 502 (2007).
[13] S. Goeb, A. De Nicola, and R. Ziessel, J. Org. Chem. **70**, 1518 (2005).
[14] A. D. Becke, J. Chem. Phys. **98**, 5648 (1993).
[15] E. Runge and E. K. U. Gross, Phys. Rev. Lett. **52**, 997 (1984).
[16] R. Bauernschmitt and R. Ahlrichs, Chem. Phys. Lett. **256**, 454 (1996).
[17] T. Yanai, D. P. Tew, and N. C. Handy, Chem. Phys. Lett. **393**, 51 (2004).
[18] K. Aidas, A. Møgelhøj, E. J. K. Nilsson, M. S. Johnson, K. V. Mikkelsen, O. Christiansen, P. Söderhjelm, and J. Kongsted, J. Chem. Phys. **128**, 194503 (2008).
[19] T. Liu and A. Troisi, J. Phys. Chem. C **115**, 2406 (2011).
[20] C. Zhao, Z. Wang, K. Zhou, H. Ge, Q. Zhang, L. Jin, W. Wang, and S. Yin, Acta Chim. Sinica **74**, 251 (2016).
[21] T. Lu and F. Chen, J. Comp. Chem. **33**, 580 (2012).
[22] T. Lu and F. Chen, J. Mol. Graph. Model. **38**, 314 (2012).
[23] M. J. Frisch, G. W. Trucks, H. B. Schlegel, G. E. Scuseria, M. A. Robb, J. R. Cheeseman,G. Scalmani, V. Barone, B. Mennucci, G. A. Petersson, H. Nakatsuji, M. Caricato, X. Li, H. P. Hratchian, A. F. Izmaylov, J. Bloino, G. Zheng, J. L. Sonnenberg, M. Hada, M. Ehara, K. Toyota, R. Fukuda, J. Hasegawa, M. Ishida, T. Nakajima, Y. Honda, O. Kitao, H. Nakai, T. Vreven, J. J. A. Montgomery, J. E. Peralta, F. Ogliaro, M. Bearpark, J. J. Heyd, E. Brothers, K. N. Kudin, V. N. Staroverov, R. Kobayashi, J. Normand, K. Raghavachari, A. Rendell, J. C. Burant, S. S. Iyengar, J. Tomasi, M. Cossi, N. Rega, J. M. Millam, M. Klene, J. E. Knox, J. B. Cross, V. Bakken, C. Adamo, J. Jaramillo, R. Gomperts, R. E. Stratmann, O. Yazyev, A. J. Austin, R. Cammi, C.Pomelli, J. W. Ochterski, R. L. Martin, K. Morokuma, V. G. Zakrzewski, G. A. Voth, P. Salvador, J. J. Dannenberg, S. Dapprich, A. D. Daniels, O. Farkas, J. B. Foresman, J. V. Ortiz, J. Cioslowski, and D. J. Fox, *Gaussian 09, Revision A.02*, Wallingford, CT, USA: Gaussian Inc. (2009).
[24] L. Zheng, Q. Zhou, X. Deng, M. Yuan, G. Yu, and Y. Cao, J. Phys. Chem. B **108**, 11921 (2004).
[25] X. Wang, Y. Guo, Y. Xiao, L. Zhang, G. Yu, and Y. Liu, J. Mater. Chem. **19**, 3258 (2009).
[26] M. C. Scharber, D. Mhlbacher, M. Koppe, P. Denk, C. Waldauf, A. J. Heeger, and C. J. Brabec, Adv. Mater. **18**, 789 (2006).
[27] J. C. Hummelen, B. W. Knight, F. LePeq, F. Wudl, J. Yao, and C. L. Wilkins, J. Org. Chem. **60**, 532 (1995).
[28] Z. Xu, L. M. Chen, M. H. Chen, G. Li, and Y. Yang, Appl. Phys. Lett. **95**, 013301 (2009).
[29] P. K. Nayak and N. Periasamy, Org. Electron. **10**, 1396 (2009).
[30] P. E. Schwenn, P. L. Burn, and B. J. Powell, Org. Electron. **12**, 394 (2011).
[31] B. P. Rand, J. Genoe, P. Heremans, and Poortmans, J. Prog. Photovolt: Res. Appl. **15**, 659 (2007).
[32] J. E. Norton and J. L. Brédas, J. Am. Chem. Soc. **130**, 12377 (2008).
[33] Y. Li, T. Pullerits, M. Zhao, and M. Sun, J. Phys. Chem. C **115**, 21865 (2011).
[34] P. Peumans, A. Yakimov, and S. R. Forrest, J. Appl. Phys. **93**, 3693 (2003).
[35] N. Bérubé, V. Gosselin, J. Gaudreau, and M. Côté, J. Phys. Chem. C **117**, 7964 (2013).
[36] X. Liu, W. Shen, R. He, Y. Luo, and M. Li, J. Phys. Chem. C **118**, 17266 (2014).
[37] X. Guo, N. Zhou, S. Lou, J. Smith, D. Tice, J. Hennek, R. Ortiz, J. T. L. Navarrete, S. Li, J. Strzalka, L. Chen, R. P. H. Chang, A. Facchetti, and T. J. Marks, Nat. Photonics. **7**, 825 (2013).
[38] D. Gupta, S. Mukhopadhyay, and K. Narayan, Sol. Energy Mater. Sol. Cells. **94**, 1309 (2010).
[39] Y. Zhou, C. Fuentes-Hernandez, J. W. Shim, T. M. Khan, and B. Kippelen, Energy Environ. Sci. **5**, 9827 (2012).
[40] X. Liu, C. Huang, W. Shen, R. He, and M. Li, J. Mol. Model. **22**, 15 (2016).
[41] M. A. Green, Solid-State Electron. **24**, 788 (1981).
[42] B. Kippelen and J. L. Brédas, Energy Environ. Sci. **2**, 251 (2009).
[43] S. Ardo and G. J. Meyer, Chem. Soc. Rev. **38**, 115 (2009).

DOI:10.1063/1674-0068/30/cjcp1702016 ©2017 Chinese Physical Society

[44] G. P. Smestad and M. Grätzel, J. Chem. Educ. **75**, 752 (1998).
[45] R. A. Marcus, Rev. Mod. Phys. **65**, 599 (1993).
[46] R. A. Marcus, Ann. Rev. Phys. Chem. **15**, 155 (1964).
[47] V. Lemaur, M. Steel, D. Beljonne, J. L. Brédas, and J. Cornil, J. Am. Chem. Soc. **127**, 6077 (2005).
[48] O. F. Mossotti, Memorie Mat. Fis. Modena **24**, 49 (1985).
[49] D. Y. Zang, F. F. So, and S. R. Forrest, Appl. Phys. Lett. **59**, 823 (1991).
[50] G. Brocks, J. van den Brink, and A. F. Morpurgo, Phys. Rev. Lett. **93**, 146405 (2004).
[51] V. D. Mihailetchi, J. K. J. van Duren, P. W. M. Blom, J. C. Hummelen, R. A. J. Janssen, J. M. Kroon, M. T. Rispens, W. J. H. Verhees, and M. M. Wienk, Adv. Funct. Mater. **13**, 43 (2003).
[52] M. Malagoli and J. L. Brédas, Chem. Phys. Lett. **327**, 13 (2000).
[53] V. Lemaur, D. A. da Silva Filho, V. Coropceanu, M. Lehmann, Y. Geerts, J. Piris, M. G. Debije, A. M. van de Craats, K. Senthilkumar, L. D. A. Siebbeles, J. M. Warman, J. L. Brédas, and J. Cornil, J. Am. Chem. Soc. **126**, 3271 (2004).
[54] M. X. Zhang, S. Chai, and G. J. Zhao, Org. Electron. **13**, 215 (2012).
[55] R. A. Marcus, J. Chem. Phys. **43**, 679 (1965).
[56] H. A. Lorentz, Ann. Phys. **9**, 641 (1880).
[57] L. Lorenz, Ann. Phys. **11**, 70 (1880).
[58] S. Yin, Y. Yi, Q. Li, G. Yu, Y. Liu, and Z. Shuai, J. Phys. Chem. A **110**, 7138 (2006).
[59] A. Troisi and G. Orlandi, J. Phys. Chem. A **110**, 4065 (2006).
[60] Y. Song, C. Di, X. Yang, S. Li, W. Xu, Y. Liu, L. Yang, Z. Shuai, D. Zhang, and D. Zhu, J. Am. Chem. Soc. **128**, 15940 (2006).
[61] J. Huang and M. Kertesz, Chem. Phys. Lett. **390**, 110 (2004).
[62] S. Yin, L. Li, Y. Yang, and J. R. Reimers, J. Phys. Chem. C **116**, 14826 (2012).
[63] T. Liu and A. Troisi, Adv. Mater. **25**, 1038 (2013).
[64] A. Listorti, B. O'Regan, and J. R. Durrant, Chem. Mater. **23**, 3381 (2011).
[65] J. W. Arbogast, C. S. Foote, and M. Kao, J. Am. Chem. Soc. **114**, 2277 (1992).
[66] P. M. Allemand, C. K. Khemani, A. Koch, F. Wudl, K. Holczer, S. Donovan, G. Grner, and J. D. Thompson, Science. **253**, 301 (1991).
[67] A. Einstein, Ann. Phys. **17**, 549 (1905).
[68] M. van Smoluchowski, Ann. Phys. **21**, 756 (1906).
[69] J. D. Huang, S. H. Wen, W. Q. Deng, and K. L. Han, J. Phys. Chem. B **115**, 2140 (2011).
[70] Q. Peng, Y. Yi, Z. Shuai, and J. Shao, J. Am. Chem. Soc. **129**, 9333 (2007).

DOI:10.1063/1674-0068/30/cjcp1702016 ©2017 Chinese Physical Society